WB3595 Final Report Group 1

Scaling Up Electrolysis: Multiphase and Heat Transfer Problems

Frederieke Backelandt 4978501
Pepijn van den Bent 4660390
Rohit Bissumbhar 4565606
Wout Dekkers 4928377
Dirk Jacobs 4872509

Design Project
TU Delft
Faculty of Mechanical, Maritime and Materials Engineering,
Minor ELECS

Delft, 18 January 2021
Teachers:
Dr. L. Botto,
Dr. R. Kortlever,
Prof.dr.ir. J.T. Padding

Contents

Nomenclature

Abbreviations

CO_2	Carbon-dioxide
GDE	Gas diffusion electrodes
H_2	Hydrogen
H_2O	Water
O_2	Oxygen

Latin letters

a,b	constants in the Tafel equation describing polarization overvoltage
E	voltage applied to the cell
E_d	decomposition overpotential
E^0	standard reversible potential
E'	voltage drop in the two-phase electrolyte
ΔE	sum of ΔE_p and ΔE_D
ΔE_d	water decomposition potential
ΔE_p	electrode polarization overvoltage
ΔG	Change in Gibbs free energy
I	integral of the nondimensional current density defined in Eq. 3.3
L	electrolyzer cell height
M	atomic weight
r_f	liquid electrolyte resistivity
r_{tp}	resistivity of the two-phase bubble layer
R_t	total cell transverse resistance
R_c	ohmic resistance
R_m	membrane resistance
T	temperature
V	fluid velocity
y	channel thickness
z	vertical coordinate

Greek letters

α	void fraction based on channel thickness
α'	void fraction based on bubble layer thickness
α_k	charge transfer coefficient
γ	constant used in equation 3.3
Γ_0	non-dimensional parameter defined by equation
δ	bubble layer thickness
ϵ_g	valence upon electrolytic decomposition
λ_g	electrochemical equivalent
μ	viscosity
ξ	axial position coordinate
ρ	density
σ	slip ratio or phase velocity ratio
τ	wall shear stress
ϕ	current density
Φ	viscous dissipation function

Subscripts

0	channel inlet conditions
1	anode side
2	cathode side
g	gas
f	liquid

Superscripts

0	non dimensional quantity

Constants

F	Faraday constant (96 485.3365 A s mol^{-1})
R	universal gas constant (8.314462618 J K^{-1} mol^{-1})

Introduction

In the 21st century, it is hard to imagine a future society without wind farms and solar panels. More and more new renewable energy sources are entering the market, aiming to supply the world with clean energy. With the growing renewable energy sources, a significant problem is rising: the intermittency of renewable energy. Wind energy farms produce different amounts of power with different wind velocities, while on the other hand, solar energy depends on solar intensity. As renewable energy sources are increasingly replacing fossil fuels, it is necessary to invent processes which provide society with continuous renewable energy.

One way of mitigating the intermittency of renewable energy is storing it in chemical bonds by using large-scale electrolysis plants. For decades, electrolysis has been studied, mostly on a small scale, and widely used in the chemical industry. This project aims to develop a numerical model for the current distribution in a gas evolving electrode, based on average two-phase flow equation and give an indication on how to include the temperature dependence. This is the first step to fully model a gas evolving electrolyser. This model would help find technical problems within the cell on a large scale and solve them.

A basic model with these processes enables analysing "what if" questions and can retrieve valuable pieces of information. This project is not aiming for a too detailed model, including all kind of sub-processes. Therefore some objectives have been set, listed in the list below:

- Describe how the void fraction and the current density depend on each other in an electrolyser.
- Create a numerical model in which the void fraction and the current density are connected.
- Explain in which way the temperature dependence within an electrolyser could be implemented.
- Discuss ways to improve the basic numerical model.

Before designing a numerical model, a literature study is performed. Chapter 2 will shortly summarise the relevant background information obtained from this literature study. This information is necessary for an understanding of the numerical model. Chapter 3 will discuss the steps taken to create a numerical model of an electrolysis cell. The results of this numerical model are presented in chapter 4 and will be discussed in chapter 5.

Background information

2.1 Electrochemical cells

In order to model the electrolysis cell, some basic knowledge on this topic has to be provided. In this chapter, the working principle of an electrolysis cell will be explained. The focus will be laid on the current density and the bubble formation in the cell.

Electrochemical cells can generally be divided into two types: the galvanic and the electrolytic cells. In a galvanic cell, the reaction happens spontaneously ($\Delta G < 0$) and in the electrolytic cell, energy is needed to let the reaction take place ($\Delta G > 0$). Electrolytic cells can be used to store energy, and therefore the focus in this paper will be on the electrolytic cells (Zoski, 2007).

Even though electrochemical cells come in many shapes and forms, every cell has the same essential parts. In figure 2.1 a visualisation of a general electrolytic cell is shown. The critical elements of a cell are indicated with the numbers 1 to 5.

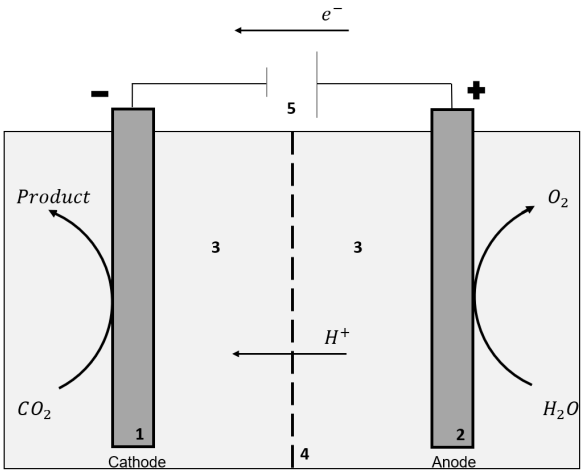

Figure 2.1: A visualisation of a electrochemical cell. The different parts of the cell are; 1: the cathode, 2: the anode, 3: the electrolyte, 4: the membrane, 5: the energy source.

These parts are present in every electrochemical cell, and they are the following:

1. **Cathode**: The cathode is the electrode where the reduction reaction occurs. This reaction takes place at the electrode-electrolyte interface and requires electrons (Bard and Faulkner, 2000). If the reactant is a gas, like in CO_2 electrolysis, a gas diffusion electrode (GDE) is used. Gas diffusion electrodes (GDE) are used in electrochemical reactions between gasses and liquids to avoid problems due to the solubility of the

gaseous reactant in the electrolyte. GDE are porous electrodes with a catalyst layer at the electrode-electrolyte interface. The gaseous reaction travels through the porous electrode towards the catalyst layer, where the reaction takes place. (Hernandez-Aldave and Andreoli, 2020). In water electrolysis, the cathode half-reaction is:

$$2\ H^+ + 2\ e^- \rightarrow\ H_2 \tag{2.1}$$

2. **Anode:** The anode is the other electrode, where the oxidation of water takes place. Both the anode and the cathode are made of highly conductive materials and are covered with a catalyst to improve the cell's performance (Bard and Faulkner, 2000). In water electrolysis, the anode half-reaction is:

$$H_2O \rightarrow \frac{1}{2}O_2 + 2H^+ + 2e^- \tag{2.2}$$

3. **Electrolyte**: An electrolyte solution is a solution that contains solvated negative and positive ions. As a result of the solvated ions, the electrolyte is able to transport electric charge through the cell. In the electrochemical cell, the electrolyte consists of two parts; the catholyte (at the cathode) and the anolyte (at the anode)(Engel and Reid, 2014). Due to the large scale continuous process, the electrolyte flows through the cell in the electrolyte channels.

4. **Membrane:** An electrochemical cell is made of two separated half cells connected by a membrane or a salt bridge. The membrane or salt bridge's function is to prevent mixing of the catholyte and the anolyte and allow the electron current to flow between the two half cells. (Engel and Reid, 2014)

5. **Energy source:** As stated at the beginning of this chapter, an electrolytic cell needs an energy source to let the reaction take place. This can be all sorts of electrical energy. In this project, surplus renewable energy is the energy source of the cell.

2.2 Heat generation within an electrolyser

As mentioned before, the problem with upscaling the electrolysis is the heat generation within the cell. Even though the goal is to develop a model for just the bubble formation, some necessary information on the heat generation within a cell will be provided to give a good recommendation on how to extend the model.

The source of heat generation are overpotentials. An overpotential η is the potential beyond a decomposition potential E_d that produces an increased thermodynamic driving force for the process. These overpotentials are not just limited to reactions, but can also be applied to different resistances in the cell processes like mass transfer limitations. All of the overpotentials express inefficiencies of the process (Stuve, 2014). Since the goal is

to derive a simple model, the concentration overpotential is left out of consideration.

Different types of overpotentials can be distinguished, and these are stated below.

- The **Ohmic overpotential** is an overpotential due to the transport of the ions between the electrodes. The resistance that these ions will endure comes out in the form of heat and can be derived from Ohm's law (Wang and Sun, 2015).
- The **electric overpotential** is caused by the resistance the electrons encounter flowing through the electrodes. Since the electrodes' material is highly conductive, this overpotential has a small contribution to the heat generation (Cretti, 2020).
- The **activation overpotential** is caused by the activation energy for the cell reaction at the electrode-electrolyte interface. The activation energy barrier is caused by multiple phenomena, such as the activation energy of the chemical reactions, the absorption and desorption mechanisms of the molecule on the electrode surface, and the molecules' rearrangement after the reaction etc (Menictas et al., 2014).
- The **concentration overpotential** is caused by the limited rate of mass transport, the product accumulates on the surface of the electrodes and creates a lack of the reactant in order for the process to continue. This phenomenon can occur when the mass transfer is relatively slow compared to the conversion (Cretti, 2020)
- the **decomposition overpotential** correlates with a increasing potential. When this occurs the anodic dissolution starts and the so-called **decomposition overpotential** is obtained (Wang and Sun, 2015).

2.3 Stating cell properties

Since the electrochemical cell and the heat generation within the cell is clear, in this section, the focus will be on the bubble formation, and the current density since those properties will be modelled.

2.3.1 Current density

To goal of this project is to model the current density for a gas evolving electrolyser. The current density is the amount of electric current flowing through a particular area. The current density is strongly dependent on the bubble formation since electric charge cannot move through a gas. In case of bubbles, the electric charge pathway is more extended, and therefore the current density will be lower. From the bottom of the cell to the top, the current density decreases (Bongenaar-Schlenter et al., 1985). A combination of dependent equations will derive the current density (ϕ). In chapter 3 this will be discussed more extensively.

2.3.2 Bubble formation

As explained earlier, the electrical resistance within the electrolysis process is partly formed by bubble formation. While the gasses hydrogen and oxygen evolve at the electrodes surface, a bubble layer is formed. To model the current distribution along the electrode it is essential to find a way to describe this phenomenon. It is called void fraction (α') which is described by equation 2.3, where y is the channel thickness and δ is the boundary thickness.

$$\alpha' = \frac{y}{\delta} \tag{2.3}$$

While a boundary layer of bubbles is formed at the electrode surface it prevents the ions from moving through the cell, so an extra resistance is generated. The bubbles start forming at the bottom of the electrode where $z = 0$ and the void fraction is also zero ($\alpha = 0$). The channel is divided in a two-phase mixture, with on the electrode side the bubbles and on the membrane site the fluid electrolyte. Mashovet's equation (eq.2.4) describes the void fraction (α') (Meredith and Tobias, 1960). The two phase resistance is thereby dependent on the voidfraction and is stated as formula 2.5, where r_f is the fluid resistivity which is temperature dependant.

$$f(\alpha') = \frac{1}{1 - 1.78\alpha' + \alpha'^2} \tag{2.4}$$

$$r_{tp} = r_f f(\alpha') \tag{2.5}$$

The total bubble resistance is therefore given by equation 2.6

$$R_t = r_{tp}\delta + r_f(y - \delta) \tag{2.6}$$

Substituting equation 2.5 into equation 2.6 gives equation 2.7

$$R_t = R_f\Big[(y - \delta) + \delta f\Big(\frac{y}{\delta}a\Big)\Big] \tag{2.7}$$

Adding the membrane resistance R_m gives the final equation for the Ohmic-overpotential as can be seen below.

$$R_c = R_1 + R_m + R_2 \tag{2.8}$$

2.3.3 The Tafel equation

The Tafel equation describes the polarisation overpotentials which occur in the electrochemical cell, stated as formula 2.9. Combined with the decomposition overpotential (ΔE_d) equation 2.10 is generated. This is used later to derive a relation between the void fraction and the current density (Funk and Thorpe, 1969).

$$\Delta E_p = a + b\ln(\phi) \tag{2.9}$$

$$\Delta E = \Delta E_{p1} + \Delta E_{p2} + \Delta E_d \tag{2.10}$$

2.3.4 Linking bubble formation and overpotentials

In order to investigate the dependency of void fraction and current density, a relation should be defined. In equation 2.11 E' is the Ohmic-overpotential, E the applied voltage and ΔE the sum of the polarisation and decomposition overpotentials which are all stated as eq. 2.13, and 2.10 (Funk and Thorpe, 1969).

$$E' = E - \Delta E \tag{2.11}$$

$$E - \Delta E = E - (\Delta E_{p_1} + \Delta E_{p_2} + \Delta E_d) \tag{2.12}$$

$$E' = \phi R_c \tag{2.13}$$

Substituting equation 2.8 and 2.10 in equation 2.11 gives the final relation 2.15. This is the equation for the electrical requirement of the cell and is one of the essential equation to derive this model (Funk and Thorpe, 1969) How the equation is used, will be explained in chapter 3.1.

$$E - (\Delta E_{p_1} + \Delta E_{p_2} + \Delta E_d) = \phi R_c \tag{2.14}$$

$$E - [(a_1 + a_2) + (b_1 + b_2)\ln\phi + \Delta E_d] = \phi\{R_m + r_f[y_1 f(\alpha_1) + y_2 f(\alpha_2)]\} \tag{2.15}$$

Creating a numerical model

A simple model for an electrolyser will be created describing void fractions, and current density distributions in a water electrolysis cell, based on an article by Funk and Thorpe, 1969. The model will be created with the help of the equations given in the article. Furthermore, our results will be compared with the article's results to verify if our model is accurate. The results from the article were experimentally checked, and they found that their model works well. The results given in the article can be seen in figure 3.1.

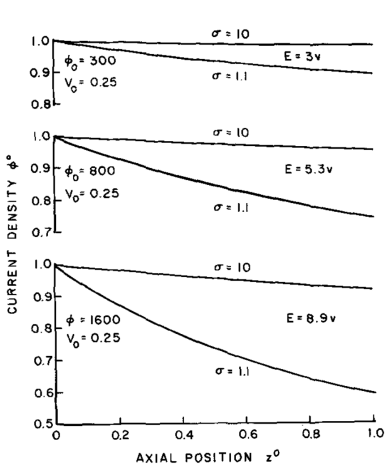

(a) The normalized current density ϕ^0 with different starting currents ϕ_0, slip ratios σ, and different voltages applied to the cell E.

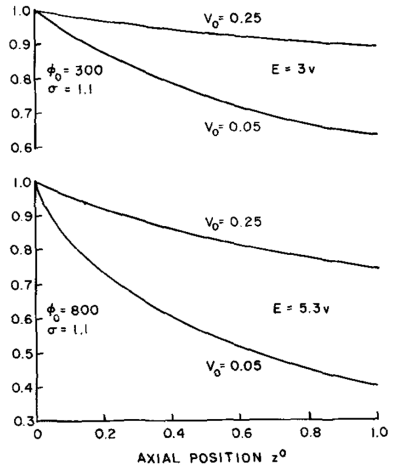

(b) The normalized current density ϕ^0 with different starting currents ϕ_0, inlet velocities V_0, and different voltages applied to the cell E.

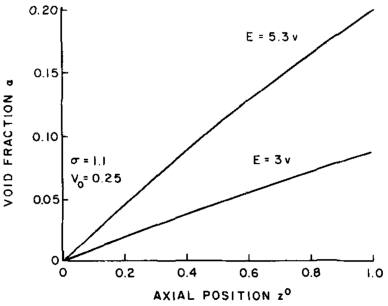

(c) The void fraction α against the normalized height z^0 for different voltages applied to the cell E.

Figure 3.1: The graphs found in the article by Funk and Thorpe, 1969. The graphs are plotted with the normalized height z^0 on the horizontal axis.

3.1 Mathematical Model

In order to create a numerical model, the mathematical model has to be understood. The current density ϕ and the void fraction α will be found by systematical solving the equation stated later in this section.

To begin with, different conservation laws have been combined in order to produce the first essential equation for the model. The conservation laws are stated in equation 3.1 (Funk and Thorpe, 1969).

$$\frac{d(\alpha\sigma y V_f)}{dz} = \frac{\lambda_g}{\rho_g}\phi \tag{3.1a}$$

$$\frac{d((1-\alpha) y V_f)}{dz} = (\gamma - 1)\phi \tag{3.1b}$$

These equations will be combined to derive the first important equation of the mathematical model, equation 3.2. This equation can be used for the cathode and anode side of the electrochemical cell.

$$\frac{\alpha}{1-\alpha} = \frac{\frac{\rho_f}{\sigma\rho_g} I}{(\gamma - 1)I + \Gamma_0} \tag{3.2}$$

This equation has only two variables, the void fraction α and the current density ϕ. To solve the equation, the calculation of the integral I, the dimensionless current density ϕ^0, the dimensionless location z^0, and Γ_0 is also required. These equations can be found in equation 3.3 from left to right.

$$I = \int_0^{z^0} \phi^0 dz^0 \qquad \phi^0 = \frac{\phi}{\phi_0} \qquad z^0 = \frac{z}{L} \qquad \Gamma_0 = \frac{y}{L}\frac{\rho_0 V_0}{\phi_0 \lambda_g} \tag{3.3}$$

In these equation ρ_f is the density of the fluid electrolyte; ρ_g the density of the gas; the slip ratio σ defined as the velocity of the gas divided by the velocity of the fluid; z the vertical axis; L the height of the electrolyser cell; γ is -17 for the cathode and +2.125 for the anode side; ϕ_0, ρ_0, V_0 are the current density, the density, the inlet velocity when the void fraction $\alpha = 0$, and λ_g the electrochemical equivalent defined by the atomic weight of the gas divided by the electrolytic decomposition.

A second equation is needed in order to find α and ϕ. This equation is the electrical requirement of the cell, which is shown in equation 3.4

$$E - [(a_1 + a_2) + (b_1 + b_2)\ln\phi + \Delta E_d] = \phi\{R_m + r_f[y_1 f(\alpha_1) + y_2 f(\alpha_2)]\} \tag{3.4}$$

In order to solve equation 3.4, the values of the Mashovet's equation and a, b have to be found. The Mashovet's equations is shown in equation 3.5 (first term). The a and b values are found by fitting a Tafel equation, also shown in equation 3.5 (second term), to data values found in the article. This can be seen in figures 4.1 and 4.2.

$$f(\alpha) = \frac{1}{1 - 1.78\alpha + \alpha^2} \qquad E_p = a + b\ln(\phi) \tag{3.5}$$

For equation 3.4: E the applied voltage; a and b constants depending on the electrode material, electrolyte, temperature, and pressure; ΔE_d the decomposition potential; R_m the resistance of the membrane; r_f the liquid electrolyte resistivity; y the distance form electrode to the membrane; and teh function f defined by Mashovet's equation.

By combining these equations, all variables can be found. An overview of the equations and how they are related to each other can be found in figure 3.2.

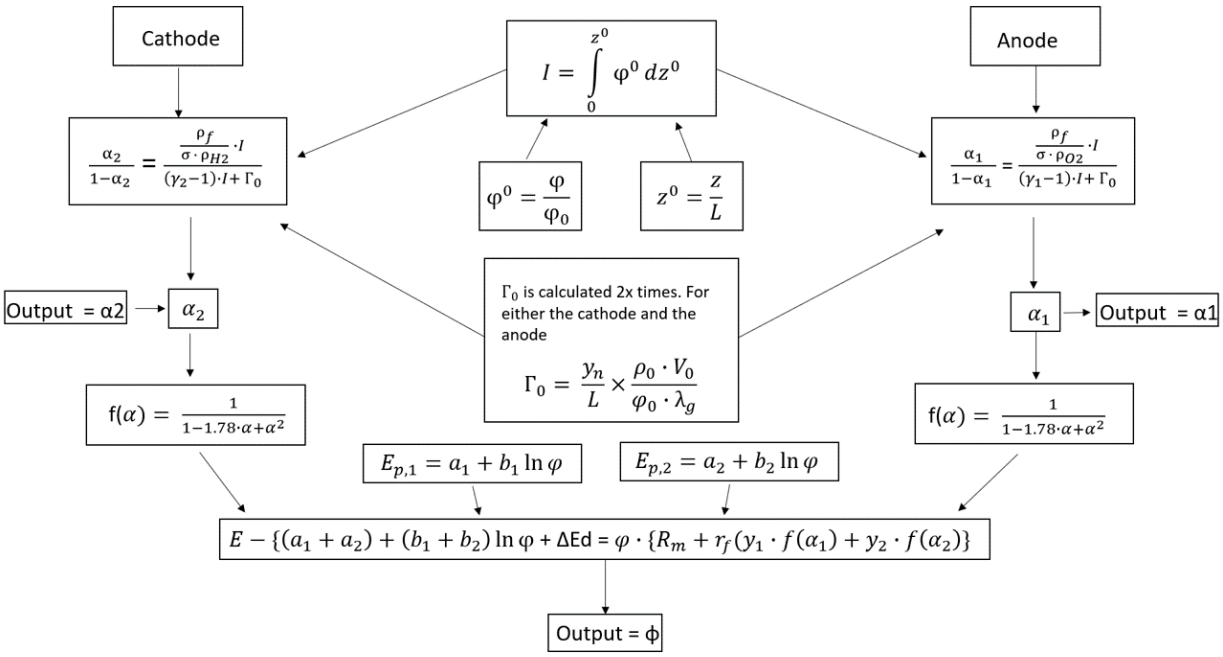

Figure 3.2: Overview of the used equation to find the current density and void fraction and how they are related to each other.

3.2 Implementation

The programming language used, to write the model, is Python 3. This because all the group members with coding experience have all worked with Python before. Another benefit of using Python is that it is an open-source software, so the model is readily accessible to everyone. The model uses multiple python packages: NumPy, 2021; SciPy, 2021b (optimize submodule SciPy, 2021a) and Matplotlib, 2021.

The algorithm models an electrolyser as seen in figure 3.3. The z axis is discretised and ranges from 0 at the bottom of the electrolyser to L at the top. The void fractions (at y_1

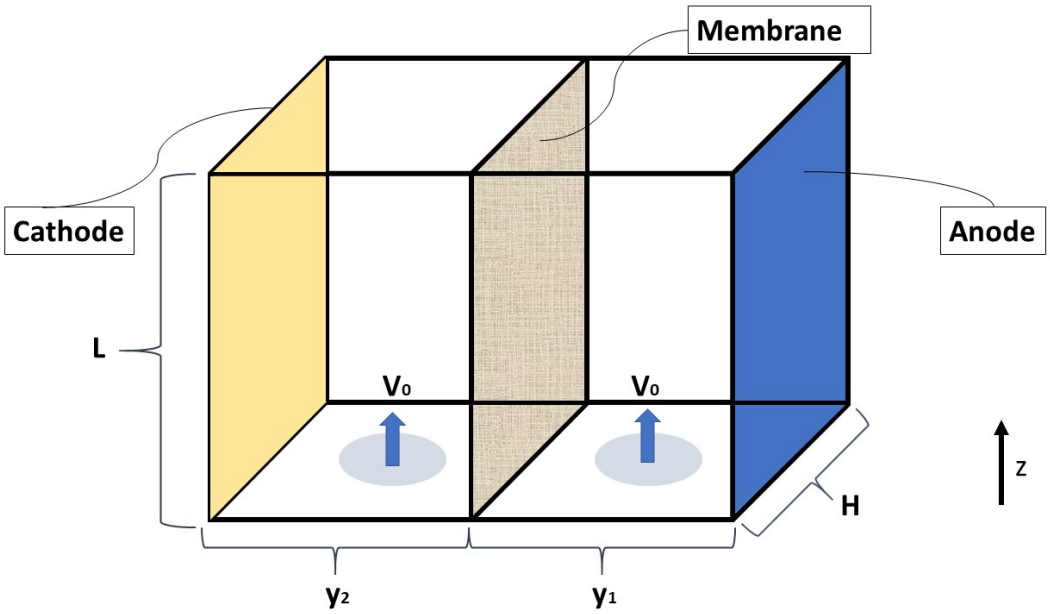

Figure 3.3: A schematic representation of the electrolyser as used in the model. z is the vertical axis, V_0 is the speed of electrolyte flow, H the width, L the height of the electrolyser, and y_2 & y_1 are the length of the sections between cathode-membrane and membrane-anode respectively.

and y_2) and the current density are calculated at discretised positions by solving a linear system of equations. The system of equations consists of equations 3.2 and 3.4, with equation 3.2 being used twice (once for the section from the anode to the membrane and again for the section from the membrane to the anode).

The algorithm first calculates the constants used in the later calculations, based on the input parameters such as the proportions of the electrolyser, the flow velocity, etc. It also determines the a and b values found in the Tafel equation (2.9) by fitting these values based on polarisation overvoltages and their corresponding current densities found in the article. The function used to do this is curve_fit and comes from the scipy.optimize submodule.

After this the system of equations is solved (using the function fsolve again from the scipy.optimise submodule) for each z position. It starts by calculating at $z = 0$ and ends at $z = L$; it does this to calculate the current density values at positions lower than the current position are necessary to calculate the current position. This is caused by the integral in equation 3.2 which can also be seen in equation 3.3.

To compute the definite integral $I = \int_0^{z^0} \phi^0 dz^0$ the trapezoidal rule was used. A definite

integral can be written as (Johnson, 2007):

$$\int_a^b f(x)dx = \frac{f(a)\Delta x}{2} + \sum_{n=1}^{N-1} f(n\Delta x)\Delta x + \frac{f(b)\Delta x}{2} \tag{3.6}$$

with $\Delta x = \frac{b-a}{N}$ and N the amount of discrete steps. The integrand is an unknown and has to be solved. To do this we use a solver and solve it for $f(b)$ and use the previously calculated values for $f(n\Delta x)$ and the starting current ϕ_0 for $f(a)$. We also change $\Delta x = \frac{b-a}{N}$ to $\Delta x = \frac{1}{N}$ as z^0 ranges from 0 to 1.

Finally we produce plots using Matplotlib such as the current density, the void fractions, and the fits used to determine the a and b values.

Results

The constants found in the Tafel equation (eq. 2.9) were fitted from data provided without using the zero data point of that data. The fitted values can be found in table 4.1. The fits themselves can be seen in figures 4.1 and 4.2.

	a	b
Anode	-0.225	0.167
Cathode	-0.328	0.137

Table 4.1: The constants in the Tafel equation (eq. 2.9) found using curve fitting.

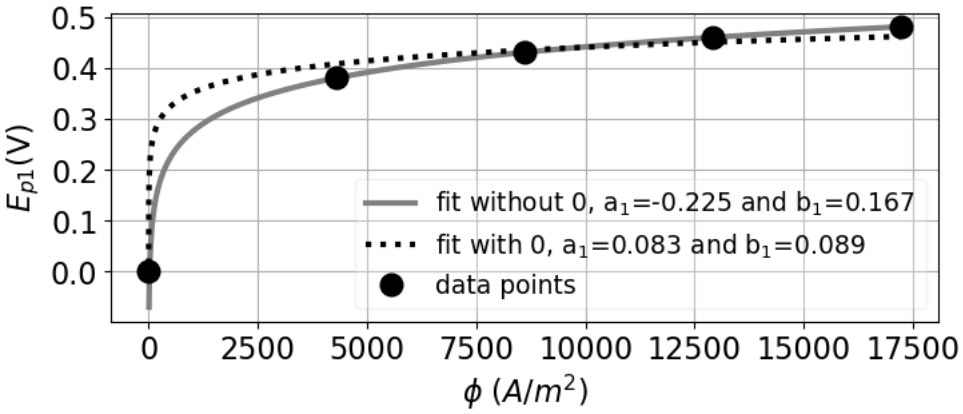

Figure 4.1: The overpotential E_{p1} in Volts against the current density ϕ in A/m^2. Two lines are fitted through the data points, one that neglects the 0 data point and one that includes a value close to zero. The values of a_1 and b_1 (anode) for the different fits can be found in the legend.

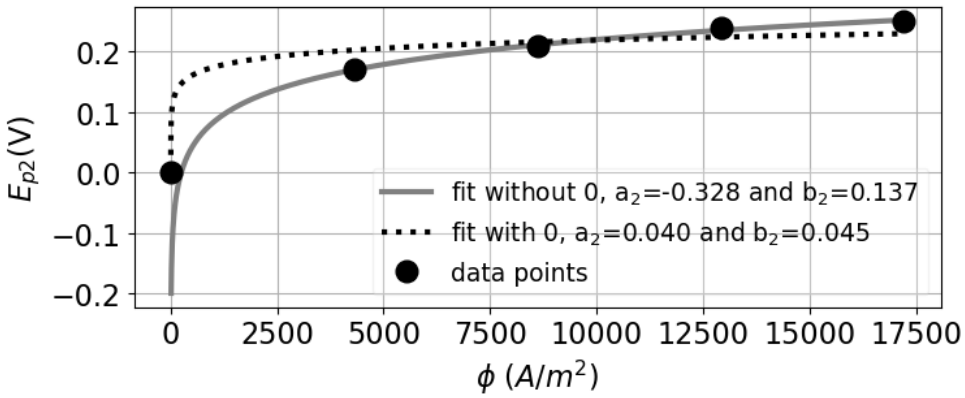

Figure 4.2: The overpotential E_{p2} in Volts against the current density ϕ in A/m^2. Two lines are fitted through the data points, one that neglects the 0 data point and one that includes a value close to zero. The values of a_2 and b_2 (cathode) for the different fits can be found in the legend.

An increase in the fluid velocity V_0 causes the void fraction to decrease, as shown in figure 4.3.

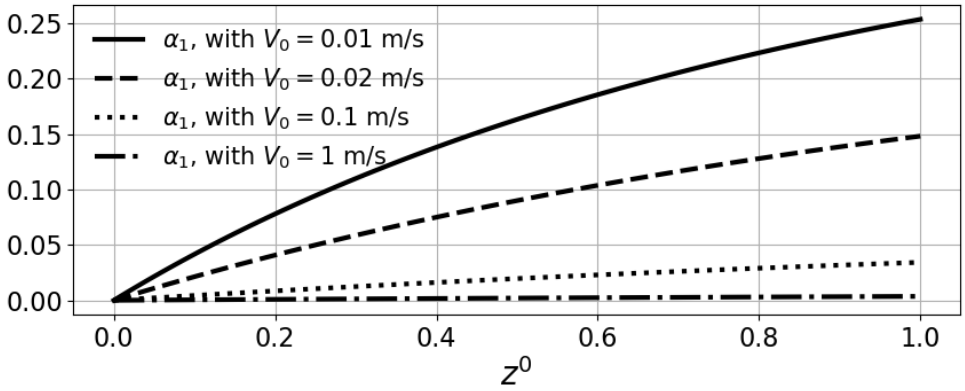

Figure 4.3: The void fraction α_1 against the normalised height z^0 for different fluid velocities. In the appendix figure 6.1 shows a similar graph for α_2.

An increase in the starting current density ϕ_0 causes the void fraction to increase, as shown in figure 4.4.

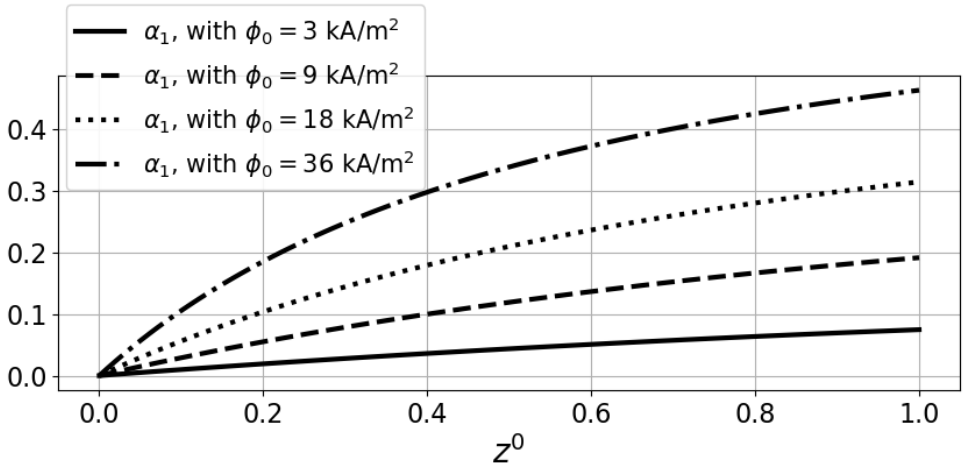

Figure 4.4: The void fraction α_1 against the normalised height z^0 for different starting current densities ϕ_0. In the appendix figure 6.2 shows a similar graph for α_2.

An increase in the pressure ϕ_0 causes the void fraction to decrease, as shown in figure 4.5.

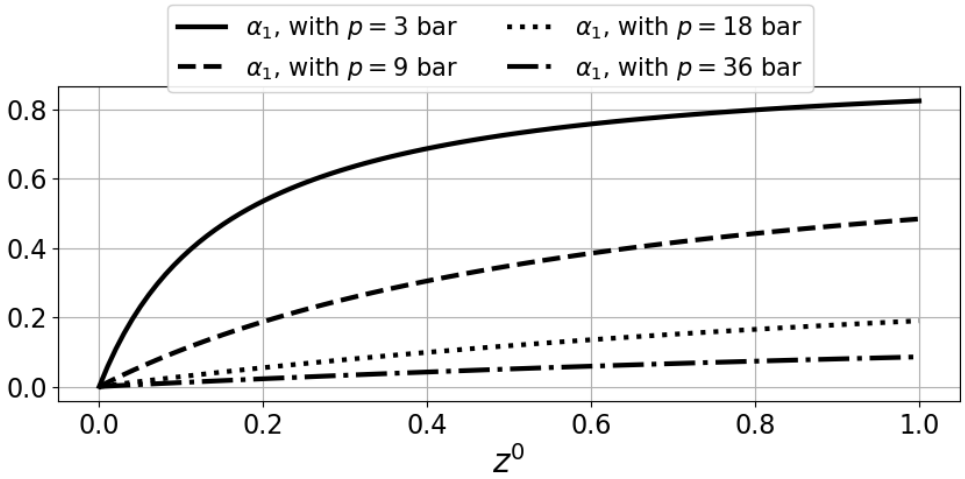

Figure 4.5: The void fraction α_1 against the normalised height z^0 at different pressures p. In the appendix figure 6.3 shows a similar graph for α_2.

From varying the ratio y_2/y_1 we can see that there is twice as much bubble in the y_2 section (where H_2 gas is produced). Figure 4.6 shows the void fractions α_1 and α_2 at different ratios, where we can see that when $y_2/y_1 = 2$ the void fractions are nearly the same.

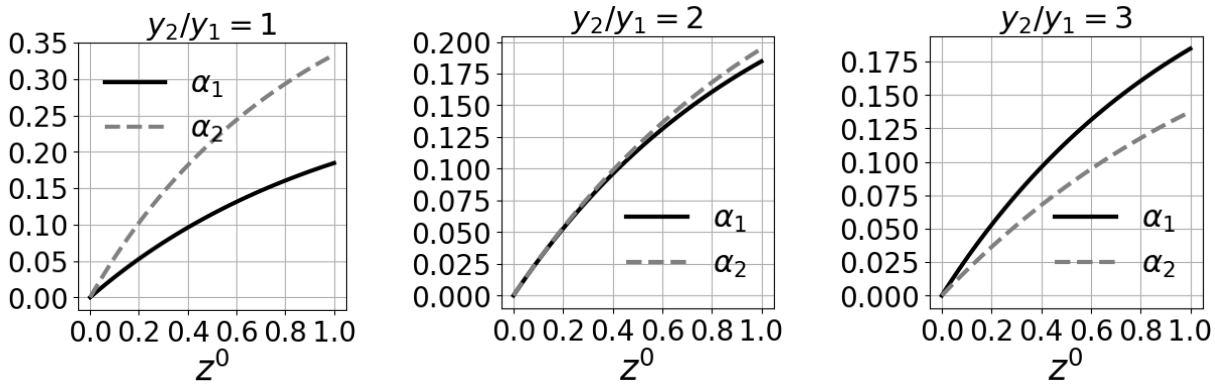

Figure 4.6: The void fractions α_1 and α_2 against the normalised height z^0 for different ratios of y_2 to y_1 as specified above the respective figure.

Increasing the width y causes the void fraction to decrease as seen in figure 4.7.

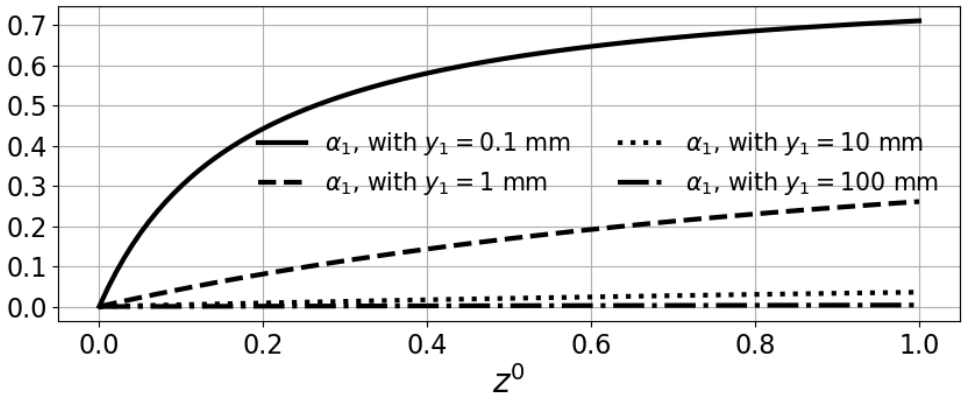

Figure 4.7: The void fraction α_1 against the normalised height z^0 for different y_1 values with $y_2/y_1 = 2$. In the appendix figure 6.4 shows a similar graph for α_2.

Increasing the height L also increases the void fractions as can be seen in figure 4.8.

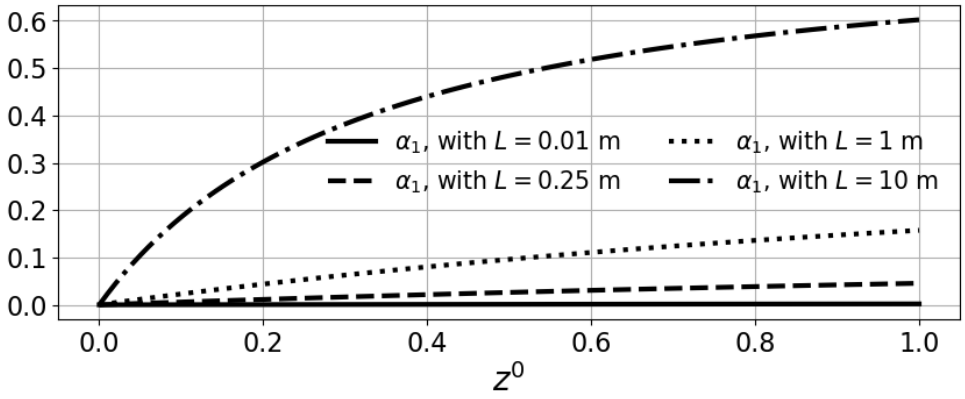

Figure 4.8: The void fraction α_1 against the normalised height z^0 for different heights L. In the appendix figure 6.5 shows a similar graph for α_2.

Discussion

5.1 Sequence of Tests

The first version of the model did not give reasonable values for the current density and the void fractions. The void fractions were too high for the input current density, and the calculated current density was zero for every z position except the input value.
To see what was going wrong with the code we assumed that the normalised current density is a decreasing straight line. First, we calculated the void fractions using equation 3.4 twice (once for each void fraction). This resulted in a reasonable shape and a correct order of magnitude for the void fractions, as shown by comparing figure 5.1 with figure 3.1c.

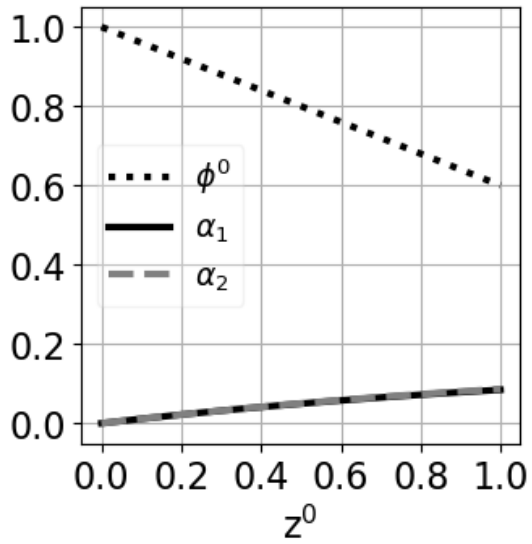

(a) The void fractions α_1 & α_2, and the ϕ^0 used to calculate them.

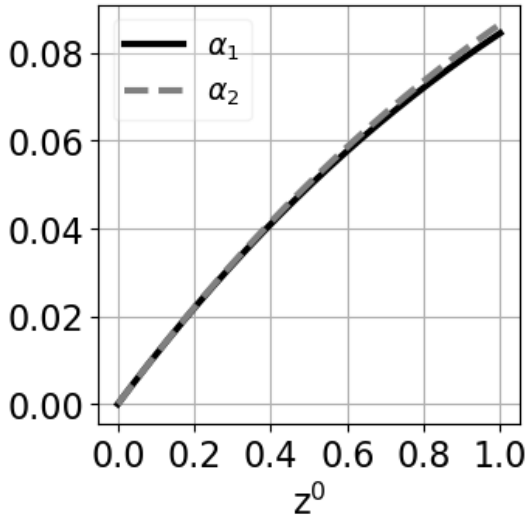

(b) The void fractions α_1 & α_2 as seen in figure 5.1a

Figure 5.1: The normalised current density ϕ^0 and void fractions α_1 & α_2 against the the normalised height z^0. Equation 3.4 was used to calculate the void fractions for a given ϕ^0.

We also tested the integral in multiple ways. First, we tested the integral on simple functions, as can be seen in figure 5.2, which were successful apart from the integral of $1/x$. The cause for this can be the way the integral is calculated. The integral equation is based on the trapezoidal rule, which uses the values of the integrand function. There might not be enough data points around 0 which could cause the error. To test this hypothesis, the step size was decreased, which resulted in the numerical solution being the same as the analytical solution. The error only occurs when the integral is calculated for values around 0, and the error does not occur on intervals between 1 and larger no matter the step size.

Afterwards, we tried to calculate the current density with the void fractions we acquired earlier, as seen in figure 5.1. This resulted in the same current density, thus signifying that the problem is not due to the integral.

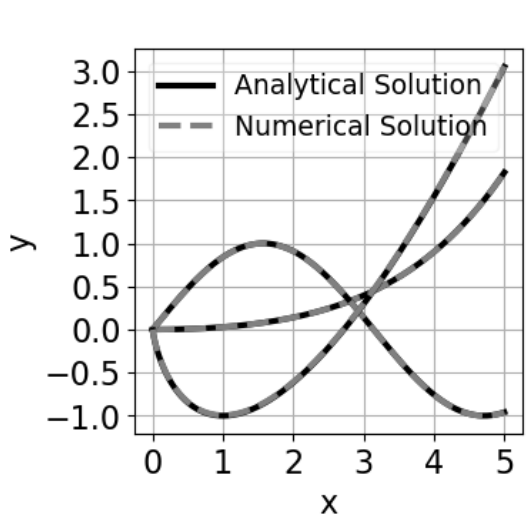

(a) The integrals of $\cos(x)$ (fast increasing at 0), a fourth order polynomial (slowly increasing at 0) and $\ln(x)$ (decreasing at 0).

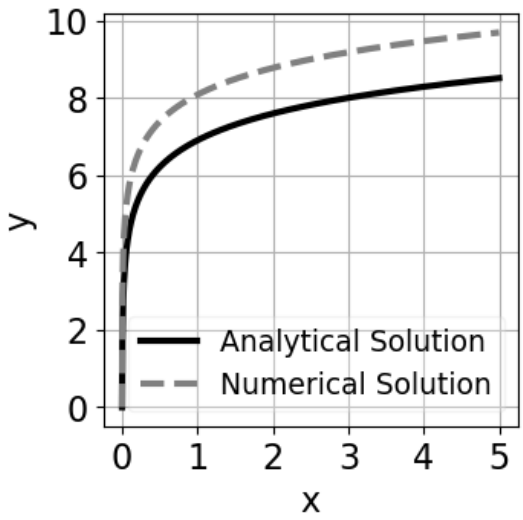

(b) The integral of $1/x$. The numerical solution and analytical solution have the same shape but a different starting position.

Figure 5.2: The graphs used in the integral tests. The horizontal axis denotes the x value and the vertical axis the y value.

Trying to solve the void fractions using both equations 3.2 and 3.4, again using the same known current density, resulted in a problem. The resulting values are not realistic, as shown in figure 5.3. The void fractions that are supposed to have a value between zero and one have negative values, and α_1 has values in the order of 10^5. This is not correct.

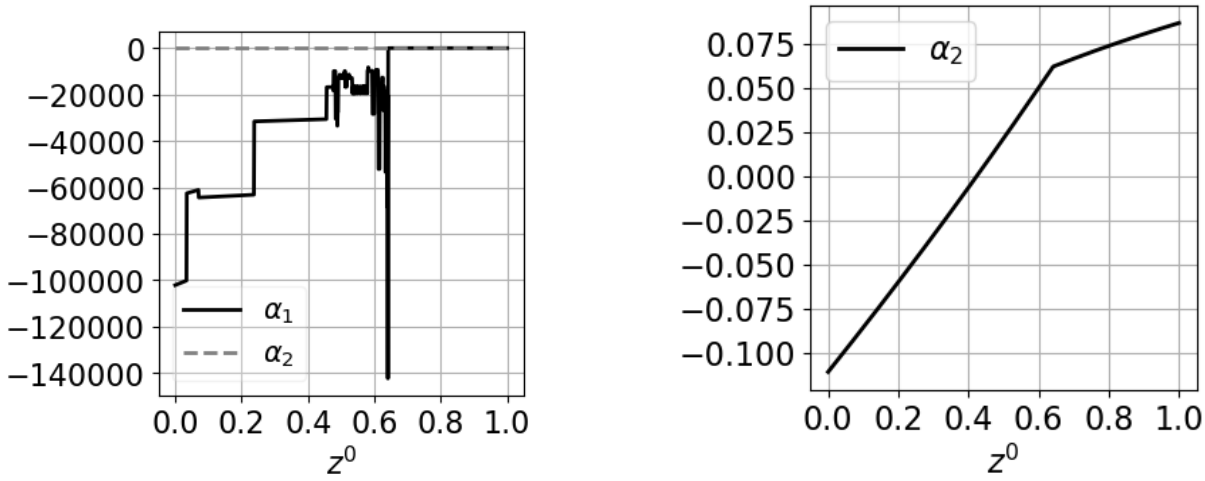

(a) The void fractions α_1 & α_2.

(b) Only the void fraction α_2.

Figure 5.3: The void fractions α_1 & α_2 against the normalised height z^0. Equation 3.2 was used to calculate the alpha values for the same given ϕ^0 seen in figure 5.1a.

From these test we can conclude the problem lies with equation 3.2. The possible causes for this could be the Mashovet's equation, the a and b constants from the Tafel equation (eq. 2.9) or the parameters used in the equation like R_m and r_f.

Mashovet's equation $f(x) = (1 - 1.78x + x^2)^{-1}$ can be used in equation 3.2 in two ways. By filling either α or $\alpha' = \alpha y/\delta$ into the equation. In our model, we used the former. Implementing the bubble layer thickness δ results in a "contraction" of the function when compared to using α instead of α'. With "contraction" we mean that the function is squeezed together as if the values corresponding to the interval (0,10) on the horizontal axis went to the interval (0,1). The bigger the delta, the more the function starts to look like the case when only α is used. This can be seen in figure 5.4. Using α' with a low delta value in Mashovet's equation causes the current density to first increase and then decrease at a higher void fraction, as shown in figure 5.5. This is unrealistic as a higher void fraction would mean a higher resistance which would cause a lower current density. Higher delta values have a more realistic value and could be a better approximation of the current density. Another problem with incorporating the delta value is that neither the value itself nor the procedure to acquire the δ value is given.

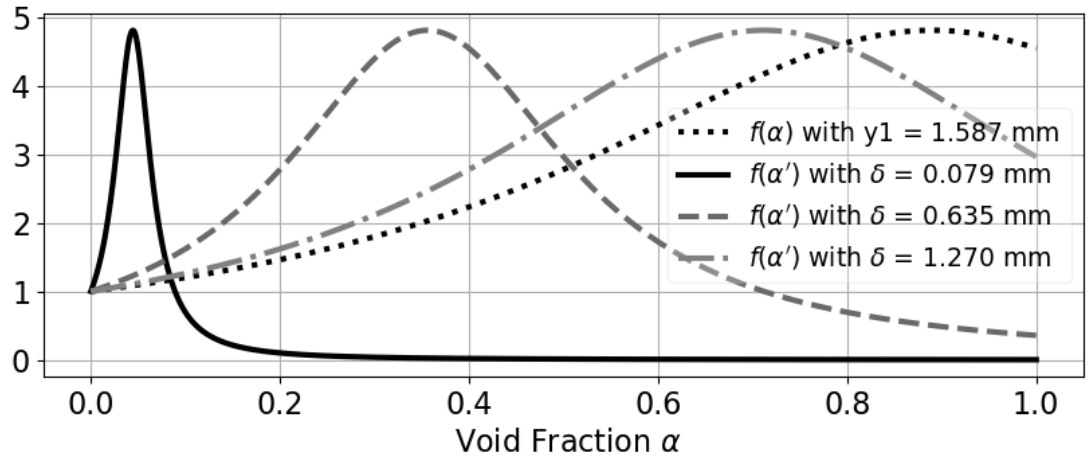

Figure 5.4: The function f described by Mashovet's equation as a function of α and $\alpha' = \alpha y/\delta$ against the void fraction α for different delta values that can be found in the legend of the figure.

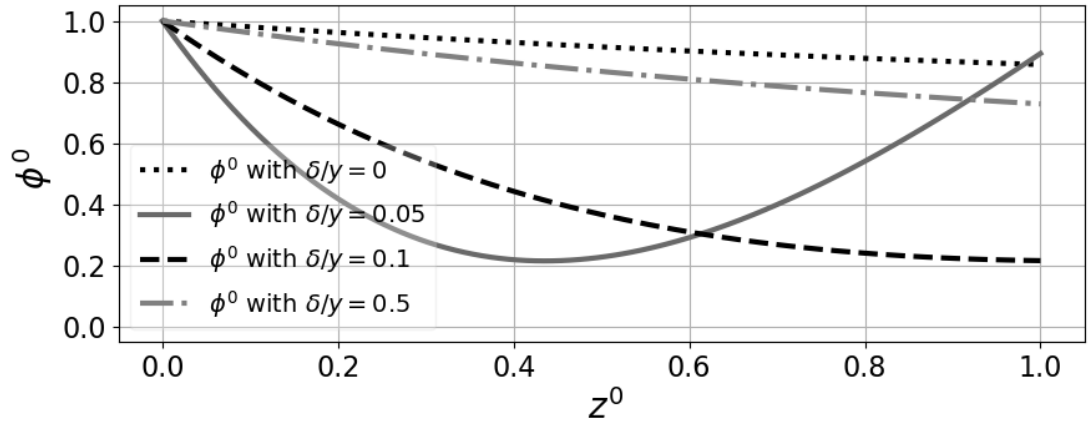

Figure 5.5: The normalized current density ϕ^0, calculated with different inputs for Mashovet's equation, against the normalised height z^0. The inputs and their specified delta values can be found in the legend of the graph.

The constants a and b in the Tafel equation $E_p = a + b \ln \phi$ were calculated by fitting to data provided in the article. The data point where the current density ϕ is zero gives an error as $\ln(0)$ is undefined. We used two methods to circumvent this problem. The first method was to neglect the data point where $\phi = 0$ and the second method was to replace data point $\phi = 0$ with a value that is close to zero. As can be seen in figures 4.1 and 4.2 the fits that do not take the zero data point into account fit the data points more but still have a tiny current when E = 0 Volt. The fit with a data point close to zero does not have the tiny current, but it does not fit the data points as well as the fit without the zero data

point. We can also see that the fit without the zero data point has negative values. When using a data point close to zero, the a and b values fluctuate a lot when moving the data point closer to zero.

The parameters, especially R_m and r_f, also influence the calculation. A mistake in the conversion to SI units is a possible explanation for the erroneous code.

5.2 Improvements

The first steps towards a model of the heat generation in a large scale CO_2 electrolyser have been taken. To improve this model further, the temperature dependence of the parameters in the model is of importance. In this chapter, the method to include the temperature in the model is described.

5.2.1 Temperature

In order to add the temperature in the model, the temperature dependence of the different parameters in the model has to be determined. In Funk and Thorpe, 1969, the current density, ϕ, and the void fraction, α, are related to the temperature in the cell by equation 5.1.

$$\rho_f V_f \frac{dT}{dz} = \frac{R\phi^2}{C_f(1-\alpha)y} + \frac{\mu\Phi}{C_f} \tag{5.1}$$

In this equation the V_f the velocity of the liquid, R the electrical resistance of the electrolyte-bubble mixture, C_f the specific heat capacity of the liquid and μ the viscosity of the liquid. Here it is assumed that the gas phase's energy transport is negligible due to the low thermal conductivity and heat capacity. For the resistance (Ohmic overpotential) the same can be said, and only the resistance of the electrolyte will experience temperature influences.

Besides the current density and the void fraction, the cell voltage, E, is dependent on the temperature as well. The general equation for the cell voltage is stated in equation 5.2 This also is the fundamental equation from which equation 2.15. As seen in 5.2, the cell voltage depends on the reaction energy, the activation overpotentials for both the cathode and the anode and the Ohmic overpotentials (Funk and Thorpe, 1969).

$$E = E_d + E_{p_1} + E_{p_2} + E_c \tag{5.2}$$

In the model E is assumed to be constant while in reality E is dependent on the temperature. This is shown by equation 5.3 where formula 5.4 is substituted for E^0 is the standard reversible potential. (Dale et al., 2008).

$$E_d = E^0 + \frac{RT}{2F} \ln\left(\frac{1.5(P - P_{H_2O})}{P_{H_2O}}\right) \tag{5.3}$$

$$E^0 = 1.5241 - 1.2261 \cdot 10^{-3} \cdot T + 1.1858 \cdot 10^{-5} \cdot T \cdot \ln(T) + 5.6692 \cdot 10^{-7} \cdot T^2 \tag{5.4}$$

In this equation, R is the gas constant, F is the Faraday constant and P is the pressure.

The activation overpotentials are calculated using the Tafel equation. A correlation to the temperature can therefore be found using equation 5.5 (Olivier et al., 2017).

$$E_p = \frac{RT}{2\alpha_k F} \ln\left(\frac{\phi}{\phi_0}\right) \tag{5.5}$$

In this equation, α_k is the charge transfer coefficient and ϕ_0 is the current exchange density.

The temperature dependence of the ohmic overpotentials are based on a fitting parameter and given in eq. 5.6 (Olivier et al., 2017), which includes the overall ohmic cell resistance. As discussed in chapter 2, the ohmic resistance times the current leads to the overall ohmic overpotential (E_c).

$$\begin{aligned} E_c = \phi(& -2.96396 - 0.02371 \cdot T + 0.12269 \cdot w + (5.7e-5) \cdot T^2 + 0.00173 \cdot w^2 \\ & + (4.7e-4) \cdot w - (3.6e-8) \cdot T^3 + (2.7e-6) \cdot w^3 - (8.9e-6) \cdot T \cdot w^2 \\ & + (2.4e-7) \cdot T^2 \cdot w) \end{aligned} \tag{5.6}$$

In this equation w is the mass concentration.

Reflection

6.1 Self Reflection

A self-reflection from each member of the group on the process over the past months.

6.1.1 First Quarter

Dirk: The first quarter of this project revolved around writing a detailed literature study, which is not exactly my expertise. The projects I had encountered as a mechanical engineering student were usually a lot more practical and revolved around building or designing things. At first, I was easily lost in all the articles and papers, but after a few weeks, I became much better in scanning the articles and finding what we needed.

Frederieke: Since I am the only chemical engineering student, a lot of the theoretical work was put on me during this part of the project. I spent a lot of time working on the theoretical background and helping the others understanding the working principle of an electrochemical cell. What I found difficult in this part of the project was that I did not have a clear view of what was expected from me in the entire quarter. We really worked from week to week instead of having a clear overall goal for the whole quarter.

Pepijn: Despite following my bachelor at the same faculty as my minor this project was very different from the projects I was used to. This because we were free to set out in the direction we desired; this was exciting but also led to unclarities. Also through a continually changing focus, it was sometimes unclear what was expected from us.

Rohit: this was a difficult subject because chemical engineering is new to me as a physics student. It was also not clear what the project's goal was in the early stages as we were mainly focused on finding a wide variety of literature regarding electrolysers. I am satisfied with what I achieved this quarter as I was able to understand the workings of an electrolyser and contributed to the literature report quite well in my view.

Wout: As a Maritime Engineering student, the topic of this project was very new for me. In the first quarter, I was able to read myself into the subject quickly. I learned many new things, but because everything was new to me, I spent a lot of time reading and learning about electrolysers and the physics. Until now, I only did projects which were based on designing a ship. This project was the first time that I needed to research such a specific subject in detail.

6.1.2 Second Quarter

Dirk: For the second quarter, the focus of the project had shifted from the literature study to the programming of the numerical model. I started working on this part with confidence, through my earlier experience with python. However, this confidence quickly disappeared when we got stuck. I have not learned a lot of new commands this project. Where I improved upon is how to handle a problem that at first seems insolvable and how to systematically work towards answers.

Frederieke: Since I did not have any experience with coding, my personal goal for the quarter was to understand the basics of modeling. I tried to understand what the others were doing and help as much as I could. We started of with a lot of confidence and energy for this part of the project, but when we got stuck at the same problem for weeks I found it hard to be as confident and positive as in the beginning. We kept working hard to find the problem and improve the model, but we were still stuck at the same problem, which was frustrating. Besides that, the goal of the project had suddenly shifted, which meant parts the literature study were not relevant anymore, and this had to be rewritten. Even though this quarter worked out different then I hoped, I learned some basic about coding and learned a lot about how to isolate a code problem. Besides that, I improved my communication skills and teamwork.

Pepijn: After we finished Q1 and set some clear goals with a comprehensive paper as a guideline I was actually quite excited to start with the modeling part of the project. In the first weeks, we were heavily motivated to make some good progress, this because we experienced last quarter that more and more deadlines appear during the period. I think from week 3 we arrived at a point from where I couldn't keep up with the programming part, this was quite frustrating because programming is such a key element. After we got stuck at the code, I experienced a missing of direction. We worked hard but didn't make progress; this was really disappointing. I realise this is how real-life projects work, but after all, it was unsatisfying to be unable to deliver what was asked from us.

Rohit: Even though I initially wanted to focus on writing the report, I quickly found myself working on the model. After the code I wrote didn't work I was quite baffled about what could cause it not to work. I first started guessing what the problem was to no avail. After a conversation with the teacher, he told us to approach the errors systematically. This helped isolate the problem(s) in the code. This way of coding is, in my opinion, the most important thing I learned during the project. I think I performed quite well this quarter. I worked a lot on the code and the report.

Wout: The second quarter was a strange one for me. I did a lot of work in the first half of the second quarter. I understood the basic model and spent a lot of time trying to get the code working. I improved my skills with python and learned how to program a basic model of an electrolyser. This changed when Corona hit our family. First I was sick, and

later I lost someone who was very dear to me. Due to Corona, I missed the motivation for this project in December. Fortunately, I was able to help the group with other assignments for other courses.

6.2 Learning points

Even though this project's main goal was to create a numerical model to describe the heat generation in an electrochemical cell, the goal was also to learn more about coding real problems and how to work on a code with the whole group. Most of the time was dedicated to isolating problems in the code and trying to solve those problems.

While working on the code, a problem occurred. The code gave the wrong trends and values for the current density and the void fraction, but the problem's source was not clear. This meant the problem had to be isolated, which we had not done before. In this project, this was one of the main learning points for the entire group.

Besides coding, progress was also made in communication, between the group members and between the group and the supervisor. While working on the project, we started documenting the progress better. A daily and weekly evaluation was introduced to document what the progress was on a daily basis and evaluate everyone's individual performance weekly.

Bibliography

Bard, A. J., & Faulkner, L. R. (2000). Introduction and overview of electrode processes. *Electrochemical methods and applications* (pp. 1–43). Wiley-Interscience.

Bongenaar-Schlenter, B. E., Janssen, L. J. J., & Van Stralen, S. J. D. (1985). The effect of the gas void distribution on the ohmic resistance during water electrolytes.

Cretti, D. (2020). *2d numerical modelling of the heat development in a co2 electrolyser* (Doctoral dissertation). TU Delft.

Dale, N., Mann, M., & Salehfar, H. (2008). Semiempirical model based on thermodynamic principles for determining 6kw proton exchange membrane electrolyzer stack characteristics. *Journal of Power Sources*, *185*(2), 1348–1353. https://doi.org/10.1016/j.jpowsour.2008.08.054

Engel, T., & Reid, P. (2014). Transport phenomena. *Physical chemistry* (pp. 969–974). Pearson Education.

Funk, J., & Thorpe, J. F. (1969). Void fraction and current density distributions in a water electrolysis cell. *Journal of The Electrochemical Society*, *116*, 48–54.

Hernandez-Aldave, S., & Andreoli, E. (2020). Fundamentals of gas diffusion electrodes and electrolysers for carbon dioxide utilisation: Challenges and opportunities. *Catalysts*, *10*(6), 713. https://doi.org/10.3390/catal10060713

Johnson, S. G. (2007). *Notes on the convergence of trapezoidal-rule quadrature*. http://dedekind.mit.edu/~stevenj/trapezoidal.pdf

Matplotlib. (2021). Matplotlib: Visualization with python. https://matplotlib.org/index.html

Menictas, C., Skyllas-Kazacos, M., & Lim, T. M. (2014). Electrochemical cells for medium- and large-scale energy storage: Fundamentalsmaria skyllas-kazacos. *Advances in batteries for medium and large-scale energy storage: Types and applications* (pp. 8–12). Woodhead Publishing.

Meredith, R. E., & Tobias, C. W. (1960). Resistance to potential flow through a cubical array of spheres. *Journal of Applied Physics*, *31*(7), 1270–1273. https://doi.org/10.1063/1.1735816

NumPy. (2021). https://numpy.org/

Olivier, P., Bourasseau, C., & Bouamama, P. B. (2017). Low-temperature electrolysis system modelling: A review. *Renewable and Sustainable Energy Reviews*, *78*, 280–300. https://doi.org/10.1016/j.rser.2017.03.099

SciPy. (2021a). Optimization and root finding (scipy.optimize). https://docs.scipy.org/doc/scipy/reference/optimize.html

SciPy. (2021b). Scipy. https://docs.scipy.org/doc/scipy/reference/index.html

Stuve, E. M. (2014). Overpotentials in electrochemical cells. *Encyclopedia of Applied Electrochemistry*, 1445–1453. https://doi.org/10.1007/978-1-4419-6996-5_330

Wang, W., & Sun, C. (2015). Advances in batteries for medium and large-scale energy storage. https://www.sciencedirect.com/book/9781782420132/advances-in-batteries-for-medium-and-large-scale-energy-storage

Zoski, C. G. (2007). Fundamentals. *Handbook of electrochemistry* (pp. 3–29). Elsevier.

Appendix

Extra Results

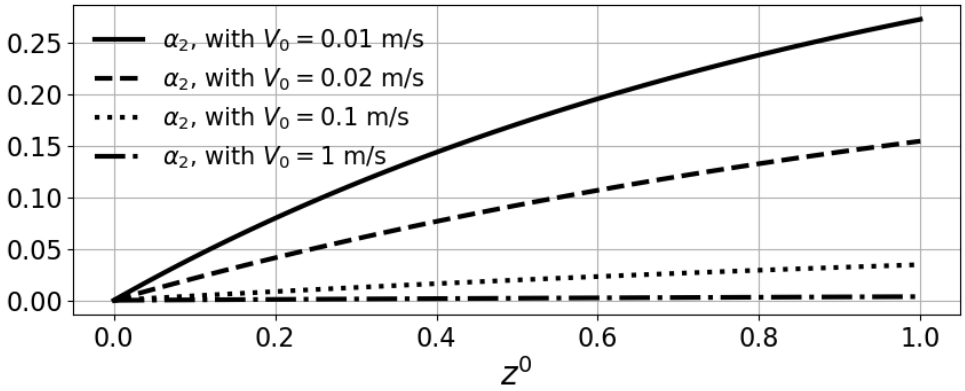

Figure 6.1: The void fraction α_2 against the normalised height z^0 for different fluid velocities.

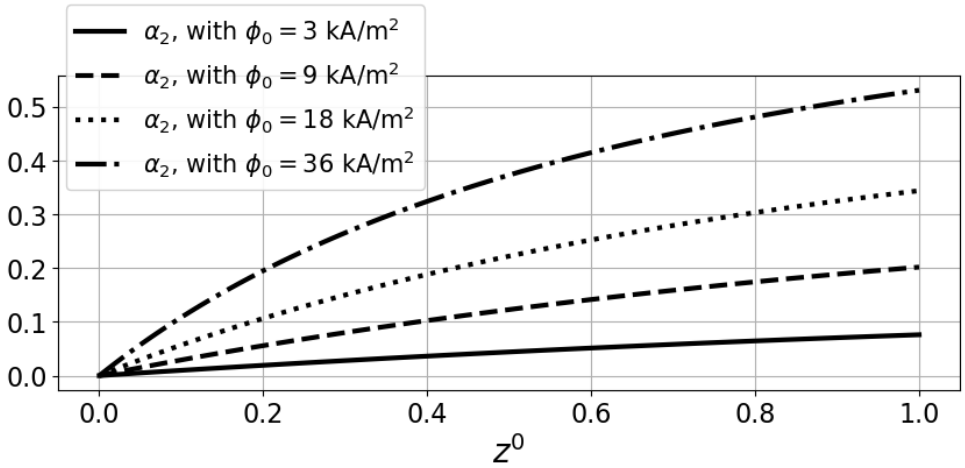

Figure 6.2: The void fraction α_2 against the normalised height z^0 for different starting current densities ϕ_0.

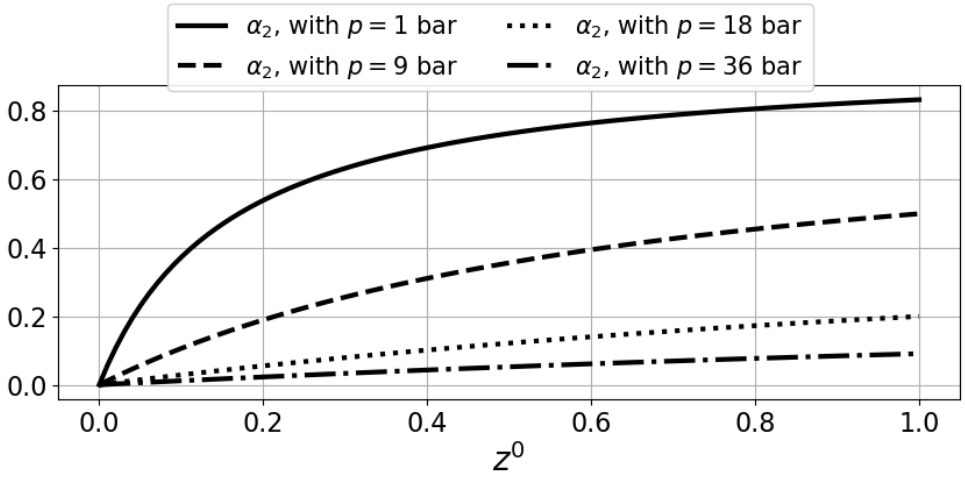

Figure 6.3: The void fraction α_2 against the normalised height z^0 at different pressures p.

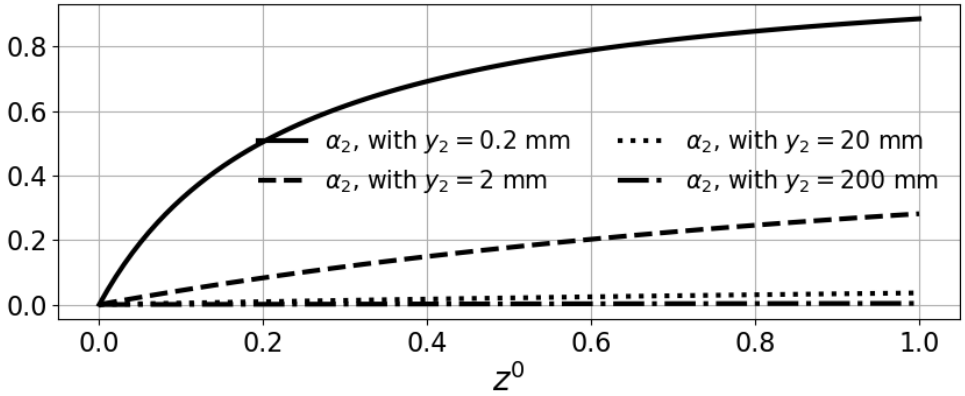

Figure 6.4: The void fraction α_2 against the normalised height z^0 for different y_2 values with $y_2/y_1 = 2$.

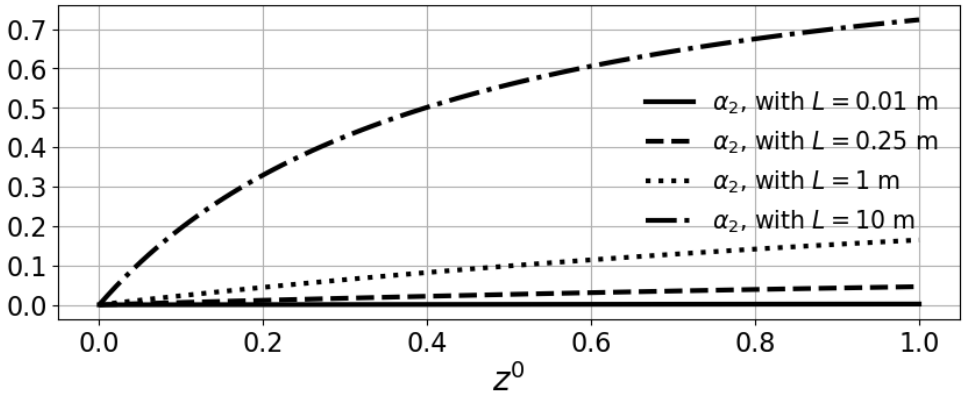

Figure 6.5: The void fraction α_2 against the normalised height z^0 for different heights L.